2022 19th International Conference on Electrical Engineering, Computing Science and Automatic Control (CCE). Mexico City, Mexico. November 9-11, 2022

Analysis of Irregular Morphologies and Mobilities of Organic Solar Cells by Simulation

I.C. Flores-Contreras
Unidad Profesional Interdisciplinaria en Ingeniería y Tecnologías Avanzadas
Instituto Politécnico Nacional
Mexico City, Mexico
ifloresc1800@alumno.ipn.mx

V. Cabrera-Arenas
Unidad Profesional Interdisciplinaria en Ingeniería y Tecnologías Avanzadas
Instituto Politécnico Nacional
Mexico City, Mexico
vcabreraa@ipn.mx

L.M. Reséndiz-Mendoza
Unidad Profesional Interdisciplinaria en Ingeniería y Tecnologías Avanzadas
Instituto Politécnico Nacional
Mexico City, Mexico
lresendiz@ipn.mx

***Abstract*—Irregular morphologies of organic solar cells with different donor:acceptor ratios and mobilities are explored. In this work, a simple algorithm that generates random disordered morphologies as a function of weight ratios from different nucleation points located randomly within the active layer and growing radially is used. By solving in two spatial dimensions the system of three coupled differential equations: Poisson's equation, and the continuity equations for the electron and hole current densities; the current density−voltage characteristics of bulk heterojunction solar cells with different donor:acceptor ratios for different mobilities are calculated. The results show that the transport properties of the materials influence the optimal value of the weight ratio of the mixture.**

Keywords—Organic solar cell, bulk-heterojunction, irregular morphology

I. Introduction

The advantages of flexibility, low cost, and easy fabrication make organic solar cells (OSCs) attractive devices as a promising future renewable energy harvester [1]. The bulk heterojunction (BHJ) architecture at nanoscale, which comprises an interpenetrating network of electron-donating and electron-accepting semiconductors to maximize the interfacial area between them, has been intensively used as the approach to overcome exciton dissociation in OSCs [2]. The ideal morphology for high-performance OSCs is the interdigitated heterojunction structure, where vertically aligned donor nanopillars are surrounded by the acceptor materials with nanoscale phase separation into de active layer, or viceversa [3]. Because difficulties in the implementation of the ideal interdigitated structure, a mixed solution deposition method is the most extensively used without limitation on the OSC efficiency [4]. In this case, active layers with irregular morphologies are obtained since the random distribution of donor and acceptor materials during solution processing [5].

When bulk heterojunctions are considered, the electric field generated at the interface of the donor and acceptor material is a key factor for optimal device performance. It is expected that the larger the interfacial area, the greater the distribution of the electric field through the active layer and therefore the greater the dissociation of excitons. In this direction, one way to adjust the interfacial area is by modifying the donor:acceptor ratio. If one material abounds more than the other, the interfacial area would be reduced, which would not be appropriate for the operation of the device, therefore, a similar proportion would seem the optimal option. However, there are experimental works that differ on this issue, some have found that the 1:1 ratio produces better performance [6], while others have found that the 7:3 ratio is better [7]. Due to the fact that different physical processes are involved in the photovoltaic process, not only the separation of the exciton influences the behavior of the device, but also the optical and their charge transport properties of each semiconductor. In order to understand in greater depth what happens in the active layer of OSCs and thus be able to improve their performance, in this work it is proposed to simulate irregular morphologies with different donor:acceptor ratios and mobilities.

II. Computational Details

A. Materials

Without loss of generality, in this work we arbitrarily consider a donor and acceptor materials, whose parameters are shown in Fig.1 and Table I. It is known that the donor material has different optical properties than the acceptor material and therefore can generate different photon absorption, in addition, photon absorption is not constant in the active layer due to optical phenomena that occur when light of the sun moves through the different layers of the device, however to simplify the analysis, the rate of generation of electron-hole pairs is assumed constant, 2.7×10^{21} cm^{-3}.

On the other hand, the width of the depletion region and the intensity of the electric field at the donor/acceptor interface were adjusted considering a doping concentration, 2.5×10^{18} cm^{-3}, so that the electric field tends to be higher at the interface than anywhere else of the active layer, as it has been shown in [8]. To analyze the effect of the transport properties of the morphologies, it is proposed to vary the mobilities of both the donor, μ_D, and the acceptor, μ_A, for three cases: $\mu_D = \mu_A$, $\mu_D < \mu_A$, and $\mu_D > \mu_A$. Although all the considerations mentioned previously to simplify our analysis do not fully represent the real situation of a solar cell, making them allows us to focus on the effect of the mobility of the materials on the parameters of the solar cell.

978-1-6654-5508-4/22/$31.00 ©2022 IEEE

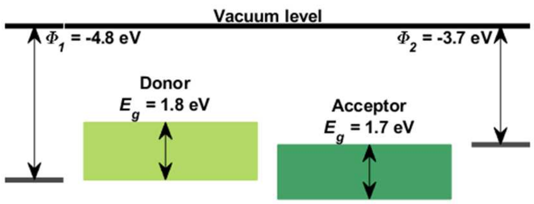

Fig. 1. Band energies of the herojunction used to simulate.

TABLE I. PARAMETERS USED IN THE 2D DRIFT-DIFFUSION SIMULATION.

Parameter	Numerical value
Dielectric constant, k	3.4
Effective density of states, N_{eff}	2.5×10^{21} cm^{-3}
Direct recombination constant, γ	1×10^{-10} cm^{3}s^{-1}

B. *Generating Irregular Morphologies*

In order to take into account the effects of the morphology of the blend, in this work, we use a simple algorithm that generates random disordered morphologies as a function of weight ratios from different nucleation points located randomly within the active layer and growing radially [9]. In Fig. 2 nine irregular morphologies with different percentages of acceptor material generated to be used in this study are shown. The devices have an active layer with 100 nm of thickness and 50 nm of lateral dimension. The anode is located at the upper boundary while the cathode is located at the lower boundary.

C. *Electrical Modeling*

The electrical modeling of organic solar cells is based on three coupled differential equations: Poisson's equation, and the continuity equations for the electron and hole current densities. Such equations for the steady-state can be expressed respectively as:

$$\nabla^2\psi = -\frac{\rho}{\varepsilon} \tag{1}$$

$$\frac{1}{q}\nabla\cdot\mathbf{J}_n = R - G \tag{2}$$

$$\frac{1}{q}\nabla\cdot\mathbf{J}_p = G - R \tag{3}$$

where q is the elementary charge, ε is the permittivity given by $\varepsilon = k\,\varepsilon_0$, where k is the dielectric constant of organic blend and ε_0 is the permittivity of vacuum, ψ is the electrostatic potential, $\mathbf{J}_{n(p)}$ is the electron (hole) current density, G is the generation rate and R is the recombination rate. By using Langevin theory, the bimolecular recombination of charge carriers is given by [10],

$$R = \gamma\left(np - n_i^2\right) \tag{3}$$

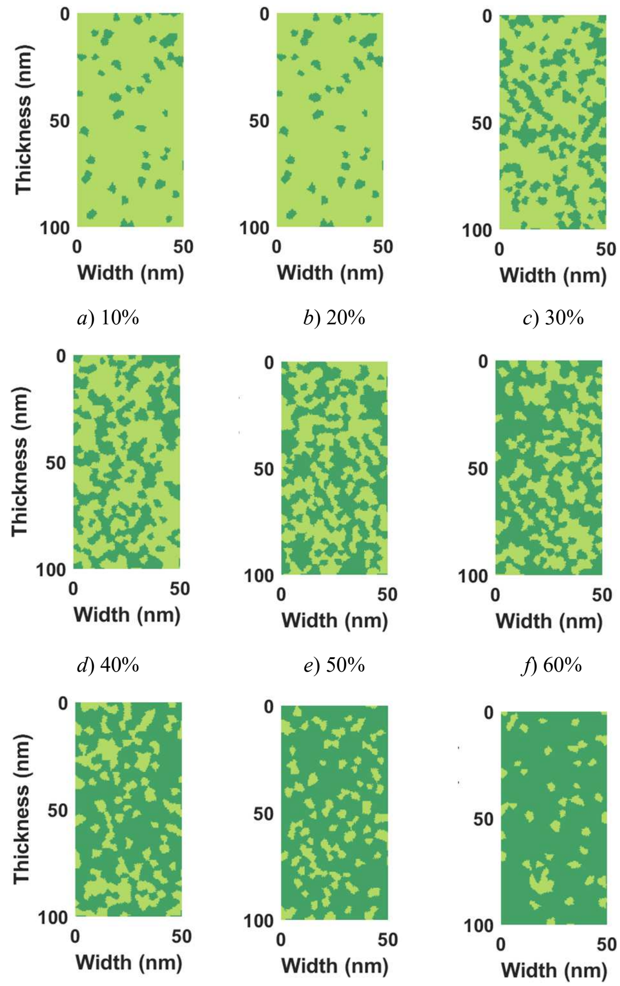

a) 10% *b*) 20% *c*) 30%

d) 40% *e*) 50% *f*) 60%

g) 70% *h*) 80% *i*) 90%

Fig. 2. Morphologies of the active layer with different percentage of acceptor material. Dark green areas correspond to acceptor phases and light green to donor phases.

where γ is the direct recombination constant, p is the hole density, n is the electron density and n_i is the intrinsic carrier density of electrons and holes. The above system is complemented by equations which describe the electron and hole concentrations and the electron and hole current densities. In this work, two spatial dimensions were used.

III. RESULTS AND DISCUSSION

A. *Case $\mu_D = \mu_A$*

First, the case in which the mobilities of both the donor and the acceptor are equal, $\mu_D = \mu_A = 1\times10^{-4}$ cm^2/V-s, is analyzed.

Fig. 3 shows the electric potential of each of the morphologies under illumination and short-circuit condition. For lower concentrations of the acceptor, it is clear that the blue color predominates, corresponding to a potential related to the position of the anode potential, while increasing the percentage, the red color related to the cathode potential predominates. To generate an electric field that dissociates the excitons inside the active layer, it is expected that the greatest potential variation occurs inside the active layer (such as in morphologies *d*, *e* and *f*), that is, away from the electrodes. The potential distribution should not obstruct the transport of carriers to their respective electrodes, so a lower potential would be expected towards the anode for holes to flow and a higher potential towards the cathode to attract electrons.

The electric field for each of the morphologies is shown in Fig. 4. Almost all morphologies show a higher electric field intensity at the interface within the active layer. The only sample that reflects an intensity predominantly close to an electrode is the sample in Fig. 4*h*.

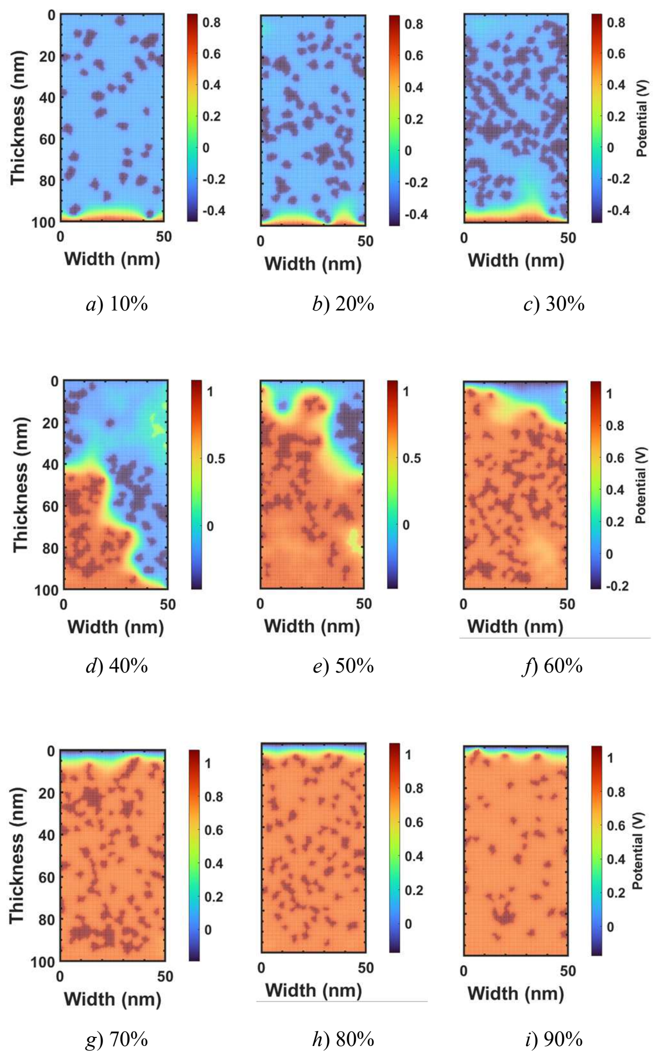

Fig. 3. Electric potential for morphology with different percentage of acceptor material under short circuit condition and $\mu_D = \mu_A$. The red and the blue colors represent the máximum and the minimum, respectively.

In Fig. 5 the current density-voltage characteristics for simulated morphologies are shown. According to these results, the best performance is obtained for the morphology with 50% of acceptor material, wich means a donor:acceptor ratio of 1:1. Due to the fact that both materials have the same transport properties, the dominance of one of the phases is not expected to produce a better performance, in this case, it can be understood that the best ratio is 1:1.

In this case, the samples with 40% and 60% of acceptor material should show a similar performance, however the first one is much better, which implies that the distribution of the phases also plays an important role.

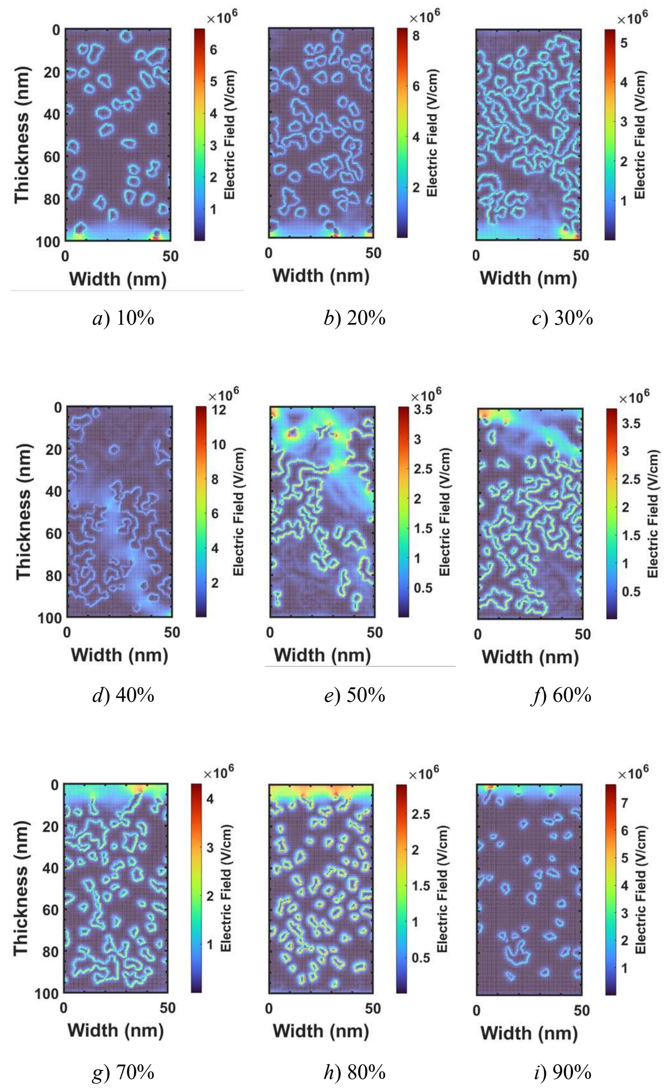

Fig. 4. Electric field for morphology with different percentage of acceptor material under short circuit condition and $\mu_D = \mu_A$. The red and the blue colors represent the máximum and the minimum, respectively.

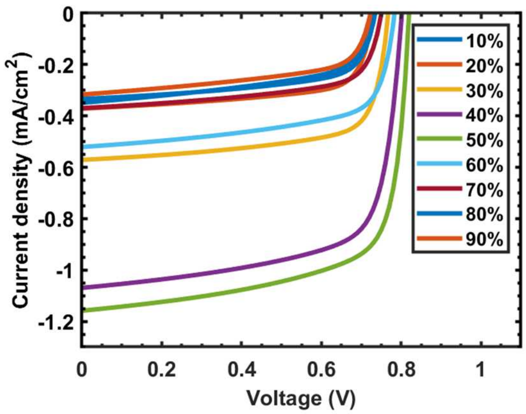

Fig. 5. Current density−voltage characteristics of bulk heterojunction solar cells with different percentage of acceptor material.

B. *Case $\mu_D < \mu_A$ and $\mu_D > \mu_A$*

In this case, other two mobilities were proposed, one lower and one higher than the previous case, that is, 1×10^{-5} cm^2/V-s and 1×10^{-4} cm^2/V-s, respectively. Fig. 6 shows the open circuit voltage (*Voc*), the short-circuit density current (*Jsc*), the fill factor (*FF*) and the maximum power (*Pmax*), which were extracted from current density-voltage characteristics, as a function of weight ratio of acceptor material for the three cases of mobility. It can be seen that all the graphs present a maximum value close to a 50% of acceptor material. Although there are few points, it is clear that *Jsc*, *FF*, and *Pmax* curves tend to move towards lower percentage of acceptor material when donor mobility are higher and viceversa. However, the *Voc* curve behaves in the opposite way, that is, the maximum occurs for a slightly higher percentage of the material that has less mobility.

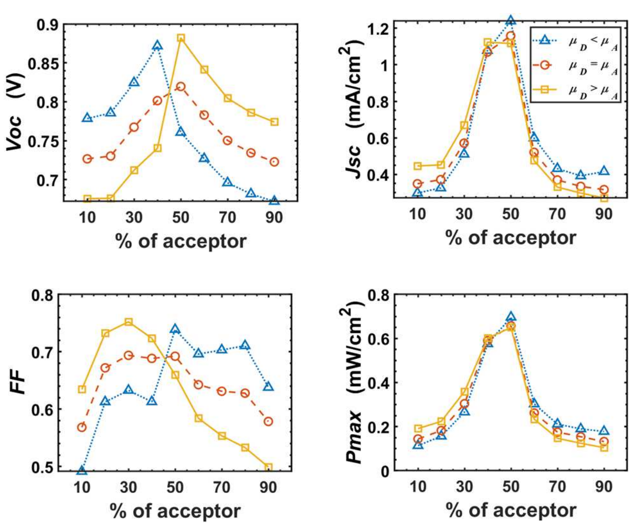

Fig. 6. Electrical parameters of the OSCs with different mobilities as a function of percentage of acceptor material.

IV. Conclusions

We have shown how mobility, when analyzed independently, can affect the optimal value of the weight ratio of an irregular morphology to obtain a better performance in the parameters of an organic solar cell. When only the mobility of the materials is considered, the best performance in the device is achieved with a morphology with a higher percentage of the material that has higher mobility. However, we make it clear that other analyzes are necessary to determine what other parameters such as the optical properties, the dielectric constant, the domain size of the morphology, and the HOMO and LUMO energy levels of the materials influence the optimal weight ratio.

Acknowledgment

This work was supported by the Instituto Politécnico Nacional under the SIP-project: 20222120.

References

[1] Kim, J. S., Park, J. H., Lee, J. H., Jo, J., Kim, D.-Y., and Cho, K., "Control of the electrode work function and active layer morphology via surface modification of indium tin oxide for high efficiency organic photovoltaics", Applied Physics Letters, vol. 91, pp. 112111, September 2007.

[2] G. Yu, J. Gao, J.C. Hummelen, F. Wudl, A.J. Heeger, "Polymer photovoltaic cells: enhanced efficiencies via a network of internal donor–acceptor heterojunctions", Science, vol. 270, pp. 1789–1791, December 1995.

[3] Yang, F., Shtein, M., and Forrest, S. R. "Controlled growth of a molecular bulk heterojunction photovoltaic cell", Nature Materials, vol. 4, pp. 37–41, January 2005.

[4] B. Ray and M. A. Alam, "Random vs regularized OPV: Limits of performance gain of organic bulk heterojunction solar cells by morphology engineering", Sol. Energy Mater. Sol. Cells, vol. 99, pp. 204–212, January 2012.

[5] Zhao, F., Wang, C., and Zhan, X., "Morphology Control in Organic Solar Cells", Advanced Energy Materials, vol. 8, pp. 1703147, October 2018.

[6] Li, G., Shrotriya, V., Huang, J., Yao, Y., Moriarty, T., Emery, K., and Yang, Y., "High-efficiency solution processable polymer photovoltaic cells by self-organization of polymer blends", Nature Materials, vol.4 , pp. 864–868, November 2005.

[7] Sun, Y., Welch, G. C., Leong, W. L., Takacs, C. J., Bazan, G. C., & Heeger, A. J., "Solution-processed small-molecule solar cells with 6.7% efficiency", Nature Materials, vol. 11, pp. 44–48, January 2012.

[8] I.C. Flores-Contreras, V. Cabrera-Arenas, L.M. Reséndiz-Mendoza, "Built-in electric field in irregular morphologies of bulk-heterojunction solar cells", 22nd International Conference on Numerical Simulation of Optoelectronic Devices, Torino, Italy, September 2022.

[9] I.C. Flores-Contreras, V. Cabrera-Arenas, L.M. Reséndiz-Mendoza, "An algorithm to generate two-dimensional morphologies of organic solar cells", 19th International Conference on Numerical Simulation of Optoelectronic Devices, Ottawa, Canada, July 2019.

[10] S. Zhou, J Sun, Ch. Zh, Z. Deng, "Comparison of recombination models in organic bulk heterojunction solar cells", Physica B, vol. 415, pp. 28-33, January 2013.